

Supporting information

I. Crystallographic Information File (CIF) for $[(\text{Ni}_2(\text{L})\text{ClO}_4)_2(\mu_2\text{-Cl})_2]^{\text{x}+}$

Table S1. Crystal Data and Structure Refinement for $[((\mu_2\text{-ClO}_4)(\text{Ni}_2(\text{L}))_2(\mu_2\text{-Cl}))_2]^{\text{x}+}$

Identification code	ni23ns	
Empirical formula	$\text{C}_{48}\text{H}_{82}\text{Cl}_{16}\text{N}_8\text{Ni}_4\text{O}_{71}\text{S}_4$	
Formula weight	2837.5	
Temperature	150(2) K	
Wavelength	0.71073 Å	
Crystal system	Triclinic	
Space group	P-1	
Unit cell dimensions	$a = 13.239(2)$ Å	$\alpha = 90.431(2)^\circ$
	$b = 13.607(2)$ Å	$\beta = 111.058(2)^\circ$
	$c = 14.751(2)$ Å	$\gamma = 90.606(2)^\circ$
Volume	2479.5(6) Å ³	
Z	1	
Density (calculated)	1.912 Mg/m ³	
Absorption coefficient	1.385 mm ⁻¹	
F(000)	1460	
Crystal size	0.28 x 0.16 x 0.12 mm ³	
Theta range for data collection	1.78 to 27.51°	
Index ranges	-16 ≤ h ≤ 16, -17 ≤ k ≤ 17, -13 ≤ l ≤ 19	
Reflections collected	15639	
Independent reflections	10919 [$R_{\text{int}} = 0.034$]	
Completeness to theta = 24.96°	95.8 %	
Absorption correction	Semi-empirical from equivalents	
Max. and min. transmission	1.000 and 0.720	
Refinement method	Full-matrix least-squares on F^2	
Data / restraints / parameters	10919 / 278 / 715	
Goodness-of-fit on F^2	1.02	
Final R indices [$I > 2\sigma(I)$]	$R_1 = 0.0588$, $wR_2 = 0.136$	
R indices (all data)	$R_1 = 0.116$, $wR_2 = 0.164$	
Largest diff. peak and hole	1.38 and -0.72 e.Å ⁻³	

II. Coordinates [\AA] of the model for $\text{Ni}_2(\text{L1})(\text{MeCN})_2$ used in the DFT calculations.

Ni	0.000000	0.000000	0.000000
S	2.368099	0.000000	-0.078061
C	2.765916	-1.105289	1.291375
C	3.879740	-0.812380	2.128325
C	4.637286	0.443526	2.068501
C	4.353974	-1.813585	3.024567
C	3.742532	-3.089635	3.125486
C	4.295651	-4.150961	4.047126
C	2.610070	-3.333340	2.305667
C	2.095585	-2.358891	1.401008
C	0.881407	-2.742890	0.657399
N	-0.023098	-1.981064	0.085618
C	-1.185520	-2.617675	-0.594060
C	-2.539433	-2.052973	-0.116939
C	-2.829665	-0.595803	-0.529584
N	-1.938662	0.394643	0.138612
H	5.655392	0.380880	2.506374
H	5.237383	-1.592016	3.648995
H	3.601197	-5.010595	4.159481
H	5.258935	-4.554722	3.649251
H	4.518224	-3.744766	5.060358
H	2.108874	-4.314987	2.371191
H	0.701241	-3.839861	0.626732
H	-1.065228	-2.452064	-1.690324
H	-1.151949	-3.718925	-0.424098
H	-2.642189	-2.172334	0.986624
H	-3.336416	-2.686425	-0.571323
H	-2.696543	-0.475893	-1.630748
H	-3.891594	-0.343987	-0.301462
S	0.515289	2.297736	-0.080997
Ni	2.605902	2.081157	0.794978
N	4.287469	1.608784	1.556825
C	-2.474732	1.438030	0.729621
C	-0.461018	2.947072	1.292102
N	2.508528	3.858747	1.477043
C	5.359768	2.654032	1.483496
C	-1.824138	2.552355	1.443080
H	-3.585692	1.488492	0.739868
C	0.071969	3.999011	2.086755
C	1.455278	4.477570	1.974038
C	3.771537	4.655161	1.369724
C	4.943757	3.992475	2.102968
H	5.604704	2.788480	0.401549
H	6.279503	2.267124	1.978209
C	-2.646517	3.275321	2.354617
C	-0.787244	4.691516	2.989341
H	1.615893	5.508576	2.352705
H	4.002053	4.761150	0.281899
H	3.593125	5.680566	1.765622
H	4.710561	3.870393	3.186054
H	5.818395	4.680837	2.044644
C	-2.155060	4.353725	3.138114
H	-3.708236	2.987706	2.453518
H	-0.375480	5.527660	3.580798
C	-3.065682	5.123920	4.065049
H	-2.498807	5.801134	4.738579
H	-3.777635	5.757776	3.481633
H	-3.687033	4.445719	4.693526
N	0.000000	0.000000	-2.099999
C	0.046552	0.117859	-3.276803

C	0.119352	0.257949	-4.724206
H	-0.332641	-0.625032	-5.232856
H	1.179685	0.342938	-5.057779
H	-0.425997	1.169905	-5.061243
N	0.023736	0.001550	2.099865
C	-0.148528	-0.183277	3.256048
C	-0.366953	-0.413751	4.679351
H	0.272934	0.258413	5.295998
H	-0.125314	-1.467114	4.951066
H	-1.430928	-0.225550	4.952521

III. The absolute sign of the nuclear quadrupole splitting

The absolute sign of the quadrupole interaction can be determined for the strongly coupled MeCN nitrogen atoms. Consider the intensity distribution of the signals in the ENDOR spectra recorded at the low-field ($g_{eff} = 2.210$) edge of the EPR spectrum, cf. figure 5. Without hyperfine semi-selection, four bands with about equal intensity are expected, as is shown in the simulation of figure 5. However, when the energy level diagram for an $S = 1/2$ system coupled to a nitrogen ($I(^{14}\text{N}) = 1$) with dominant hyperfine interaction is considered (see figure S1), only the ($\Delta M_S = \pm 1, M_I = +1$) EPR transition is resonant at the low-field edge of the EPR spectrum. Therefore, in the ENDOR spectrum, the transitions $M_I = 0 \leftrightarrow +1$, indicated in red in figure S1 will dominate and the transitions $M_I = 0 \leftrightarrow -1$ will be attenuated. This is the case for the two innermost signals in the ENDOR spectrum, and such a pattern can only be reproduced by taking a positive value for P_x in Figure S1. If P_x is negative, the outermost two signals will dominate the ENDOR spectrum. By the same arguments, the transitions $M_I = 0 \leftrightarrow -1$ will dominate the ENDOR spectrum for the magnetic field set near g_z (see Figure S1). Since the ENDOR spectrum at $g_{eff} = 2.037$ displays four signals for which the innermost two dominate the spectrum, P_z has to be negative.

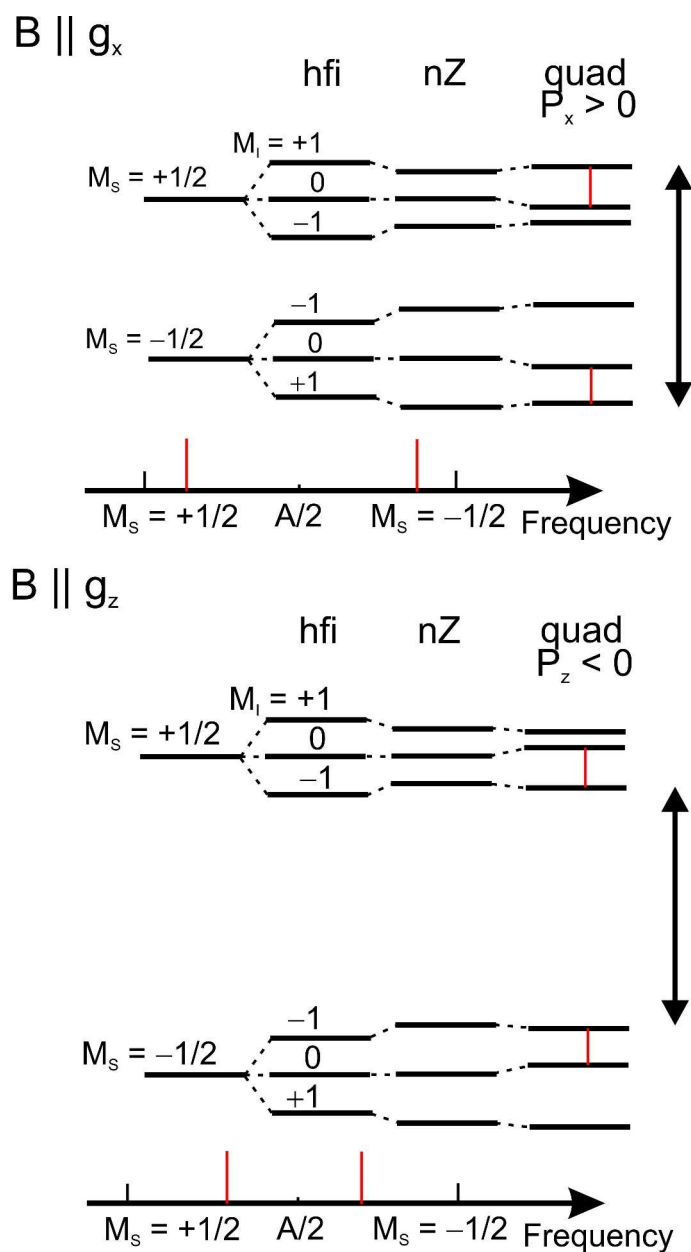


Figure S1. Energy level diagram, including electron and nuclear Zeeman, hyperfine and quadrupole interactions (not to scale) of the electron and nitrogen nuclear spin levels at low-field ($B \parallel g_x$) and high-field ($B \parallel g_z$) edge of the EPR spectrum. The vertical arrow indicates the microwave transition. At both edges, hyperfine-(semi)selection occurs and the two innermost signals in the ENDOR spectrum become dominant only for $P_x > 0$ MHz and $P_z < 0$ MHz.

IV. Hyperfine tensor for a mixed $3d_{z^2}$, $3d_{xy}$ SOMO

IV.1. Definitions

The SOMO as found in $[\text{Ni}_2\text{L}(\text{MeCN})_2]^{3+}$ is given by

$$|\Psi\rangle = A|xy\rangle + E|z^2\rangle \quad (1.1)$$

where A and E are the wavefunction coefficients. A^2 and E^2 are spin densities in the xy and z^2 orbitals.

General Slater orbital ($n = 3$) expressions for the $3d_{xy}$ and $3d_{z^2}$ orbitals

$$|xy\rangle = N_{xy}xye^{-\zeta r/na_0} = 2\sqrt{\frac{(\zeta/a_0)^7}{2\pi(3)^8}}xye^{-\zeta r/na_0} \quad (1.2)$$

$$|z^2\rangle = N_{z^2}(3z^2 - r^2)e^{-\zeta r/na_0} = \sqrt{\frac{(\zeta/a_0)^7}{2\pi(3)^9}}(3z^2 - r^2)e^{-\zeta r/na_0} \quad (1.3)$$

where ζ is the Slater exponent and N_{xy} and N_{z^2} are the normalization factors.

The anisotropic hyperfine interaction (see, e.g. Carrington, A. and McLachlan, A.D., “Introduction to magnetic resonance”, Harper and Row, New York, 1967) is given by

$$\vec{\vec{A}}(\vec{r}) = -\gamma_e\gamma_N \begin{Bmatrix} r^2 - 3x^2 & -3xy & -3xz \\ -3xy & r^2 - 3y^2 & -3yz \\ -3xz & -3yz & r^2 - 3z^2 \end{Bmatrix} \frac{1}{r^5} \quad (1.4)$$

where γ_e and γ_N are the electronic and nuclear gyromagnetic ratios. Note that the trace of (1.4) is zero.

The hyperfine tensor of the spin Hamiltonian is given by

$$\vec{\vec{A}} = \langle\Psi|\vec{\vec{A}}(\vec{r})|\Psi\rangle \quad (1.5)$$

IV.2. Hyperfine tensor for a pure $3d_{z^2}$ SOMO ($A = 0$)

For a pure $3d_{z^2}$ SOMO, equation (1.5) becomes

$$\vec{\bar{A}} = E^2 \langle z^2 | \vec{\bar{A}}(\vec{r}) | z^2 \rangle \quad (2.1)$$

The off-diagonal elements are uneven functions of x , y and/or z . Since the $3d_{z^2}$ orbital (1.3) is an even function of x , y and z , all off diagonal elements evaluate to 0. The A_{zz} term evaluates to

$$A_{zz} = -\gamma_e \gamma_N E^2 N_{z^2}^2 \left\langle \left(3z^2 - r^2 \right)^2 e^{-2\zeta r/na_0} \frac{r^2 - 3z^2}{r^5} \right\rangle \quad (2.2)$$

The integral can be evaluated after transformation into spherical coordinates

$$A_{zz} = -\gamma_e \gamma_N E^2 N_{z^2}^2 \int dr r^3 e^{-2\zeta r/na_0} \int \sin \theta d\theta \int d\phi (3 \cos^2 \theta - 1)^2 (1 - 3 \cos^2 \theta) \quad (2.3)$$

All three integrals are trivial. The ϕ integration gives 2π . The θ integral can be rewritten as

$$\int_{-1}^1 dx (1 - 3x^2)^3 = \frac{-96}{105} \quad (2.4)$$

The r integral evaluates to

$$\int dr r^3 e^{-2\zeta r/na_0} = -\left(\frac{na_0}{2}\right)^3 \frac{\partial^3}{\partial \zeta^3} \int dr e^{-2\zeta r/na_0} = -\left(\frac{na_0}{2}\right)^4 \frac{\partial^3}{\partial \zeta^3} \left(\frac{1}{\zeta}\right) = 6 \left(\frac{na_0}{2\zeta}\right)^4 \equiv P_r \quad (2.5)$$

where the r integral is abbreviated as P_r to save space in the coming formulas. Substitution of the integrals into (1.8) gives

$$A_{zz} = -\gamma_e \gamma_N E^2 \frac{(\zeta/a_0)^7}{2\pi(3)^9} P_r 2\pi \frac{-96}{105} = \gamma_e \gamma_N E^2 P_r \frac{(\zeta/a_0)^7}{(3)^8} \frac{32}{105} \quad (2.6)$$

The A_{xx} and A_{yy} elements can in principle be calculated similarly. However, it is known that the trace of the anisotropic tensor (1.4) is 0 ($A_{xx} + A_{yy} + A_{zz} = 0$) and it is trivial to see that the A_{xx} and A_{yy} terms give exactly the same integral. Thus, $A_{xx} = A_{yy} = -1/2 A_{zz}$. The total hyperfine tensor for a pure $3d_{z^2}$ SOMO becomes

$$\vec{\bar{A}} = \gamma_e \gamma_N E^2 P_r \frac{(\zeta/a_0)^7}{(3)^8} \frac{32}{105} \begin{pmatrix} -\frac{1}{2} & 0 & 0 \\ 0 & -\frac{1}{2} & 0 \\ 0 & 0 & 1 \end{pmatrix} \quad (2.7)$$

The tensor is axial and colinear with the xyz axes of the set of d orbitals.

IV.3. Hyperfine tensor for a pure $3d_{xy}$ SOMO ($E = 0$)

Now we derive the hyperfine tensor in the case of a pure $3d_{xy}$ orbital. Equation (1.5) evaluates to

$$\vec{\bar{A}} = A^2 \langle xy | \vec{\bar{A}}(\vec{r}) | xy \rangle \quad (3.1)$$

The off diagonal elements are again zero, because the integrand is an uneven function of x , y and/or z . The A_{zz} element becomes

$$A_{zz} = -\gamma_e \gamma_N A^2 N_{xy}^2 \left\langle x^2 y^2 e^{-2\zeta r/na_0} \frac{r^2 - 3z^2}{r^5} \right\rangle \quad (3.2)$$

Transformation into spherical coordinates leads to

$$A_{zz} = -\gamma_e \gamma_N A^2 N_{xy}^2 \int dr r^3 e^{-2\zeta r/na_0} \int \sin \theta d\theta \int d\varphi \sin^4 \theta \sin^2 \varphi \cos^2 \varphi (1 - 3 \cos^2 \theta) \quad (3.3)$$

The r integral is equal to (2.5) and the φ integral evaluates as

$$\int_0^{2\pi} d\varphi \sin^2 \varphi \cos^2 \varphi = \frac{\pi}{4} \quad (3.4)$$

The θ integral simplifies to

$$\int_{-1}^1 dx (1 - x^2)^2 (1 - 3x^2) = \frac{64}{105} \quad (3.5)$$

Substitution of the integrals into (3.3) followed by normalization gives

$$A_{zz} = -\gamma_e \gamma_N A^2 4 \frac{(\zeta/a_0)^7}{2\pi(3)^8} P_r \frac{16\pi}{105} = -\gamma_e \gamma_N A^2 \frac{(\zeta/a_0)^7}{(3)^8} P_r \frac{32}{105} \quad (3.6)$$

Note that except for the $-$ sign, the expression (3.6) equals (2.6). The A_{xx} and A_{yy} elements are again either evaluated similarly, or by making use of the tracelessness of (1.4). Thus, $A_{xx} = A_{yy} = -\frac{1}{2}A_{zz}$. The total hyperfine tensor for a pure $3d_{xy}$ SOMO is

$$\vec{\bar{A}} = -\gamma_e \gamma_N A^2 P_r \frac{(\zeta/a_0)^7}{(3)^8} \frac{32}{105} \begin{pmatrix} -\frac{1}{2} & 0 & 0 \\ 0 & -\frac{1}{2} & 0 \\ 0 & 0 & 1 \end{pmatrix} \quad (3.7)$$

The expressions (2.7) and (3.7) only differ in sign, and the coefficients A^2 and E^2 . The tensor is again axial and colinear with the xyz axes of the set of d orbitals.

IV.4. Hyperfine tensor for mixed $3d_{z^2}$, $3d_{xy}$ SOMO

Following the same procedure again and using (1.1) as the SOMO, equation (1.5) becomes

$$\vec{\vec{A}} = E^2 \langle z^2 | \vec{\vec{A}}(\vec{r}) | z^2 \rangle + A^2 \langle xy | \vec{\vec{A}}(\vec{r}) | xy \rangle + 2AE \langle xy | \vec{\vec{A}}(\vec{r}) | z^2 \rangle \quad (4.1)$$

The first two terms have been evaluated in sections 2 and 3. The cross term $2AE \langle xy | \vec{\vec{A}}(\vec{r}) | z^2 \rangle$ now has to be evaluated. The cross term only contributes to the A_{xy} element of (1.4), since all other elements give an integrand that is uneven with respect to either x , y or z . The A_{xy} element becomes

$$A_{zz} = -\gamma_e \gamma_N 2AEN_{xy} N_{z^2} \left\langle xy (3z^2 - r^2) e^{-2\zeta r/na_0} \frac{-3xy}{r^5} \right\rangle \quad (4.2)$$

Transformation into spherical coordinates gives

$$\begin{aligned} A_{zz} &= -\gamma_e \gamma_N 2AEN_{xy} N_{z^2} \int dr r^3 e^{-2\zeta r/na_0} \int \sin \theta d\theta \int d\varphi (-3) \sin^4 \theta \sin^2 \varphi \cos^2 \varphi (3 \cos^2 \theta - 1) \\ &= \gamma_e \gamma_N 6AEN_{xy} N_{z^2} P_r \int \sin \theta d\theta \int d\varphi \sin^4 \theta \sin^2 \varphi \cos^2 \varphi (3 \cos^2 \theta - 1) \end{aligned} \quad (4.3)$$

The θ and φ integrals equal (3.4) and minus (3.5). Thus,

$$\begin{aligned} A_{zz} &= \gamma_e \gamma_N 6AEN_{xy} N_{z^2} P_r \frac{\pi}{4} \left(-\frac{64}{105} \right) = \gamma_e \gamma_N 6AEP_r \frac{2}{\sqrt{3}} \frac{(\zeta/a_0)^7}{2\pi(3)^8} \frac{\pi}{4} \left(-\frac{64}{105} \right) \\ &= -\gamma_e \gamma_N AEP_r \sqrt{3} \frac{(\zeta/a_0)^7}{(3)^8} \frac{32}{105} \end{aligned} \quad (4.4)$$

The total hyperfine tensor becomes

$$\vec{\vec{A}} = -\gamma_e \gamma_N P_r \frac{(\zeta/a_0)^7}{(3)^8} \frac{32}{105} \begin{pmatrix} -\frac{1}{2}(A^2 - E^2) & \sqrt{3}AE & 0 \\ \sqrt{3}AE & -\frac{1}{2}(A^2 - E^2) & 0 \\ 0 & 0 & (A^2 - E^2) \end{pmatrix} \quad (4.5)$$

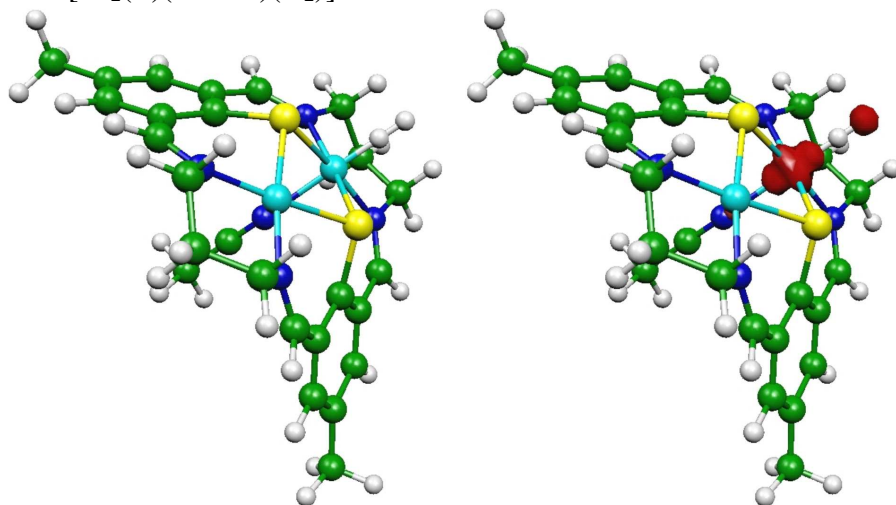
Thus, the cross term of (4.1) causes a reorientation of the principal x and y axes of $\vec{\vec{A}}$. The principal z axis remains parallel to the z axis of the $3d_{z^2}$ orbital. Diagonalization of (4.5) gives eigenvalues (denoted by primes)

$$\left\{ \begin{array}{l} A'_x = -\gamma_e \gamma_N P_r \frac{\left(\frac{\zeta}{a_0}\right)^7}{(3)^8} \frac{32}{105} \left[-\frac{1}{2} (A^2 - E^2) + \sqrt{3} AE \right] \\ A'_y = -\gamma_e \gamma_N P_r \frac{\left(\frac{\zeta}{a_0}\right)^7}{(3)^8} \frac{32}{105} \left[-\frac{1}{2} (A^2 - E^2) - \sqrt{3} AE \right] \\ A'_z = -\gamma_e \gamma_N P_r \frac{\left(\frac{\zeta}{a_0}\right)^7}{(3)^8} \frac{32}{105} (A^2 - E^2) \end{array} \right. \quad (4.6)$$

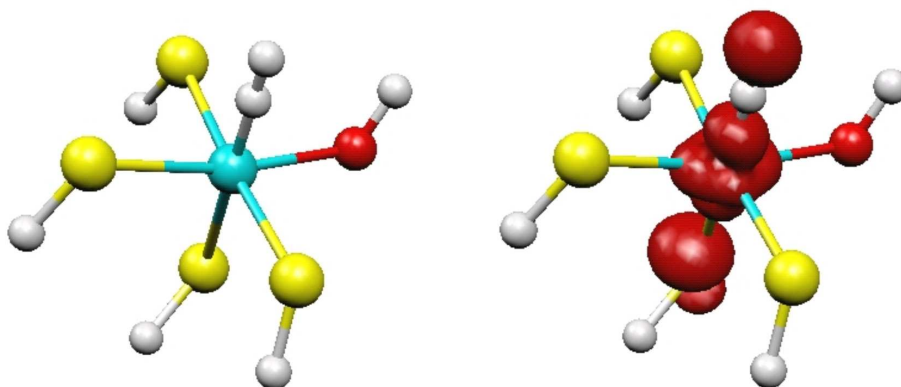
In general, the additional terms cause rhombicity, i.e., A'_x and A'_y are no longer equal. However, for the case $A = \pm\sqrt{3}E$ and $E = \pm\sqrt{3}A$, the tensor becomes axial.

V. Structures (left) and spin density plots (right) in DFT calculations with the aim to investigate the binding of H₂.

V.1. [Ni₂(L)(MeCN)(H₂)]³⁺



V.2 [Ni³⁺(SH⁻)₄(OH⁻)(H₂)]



V.3 Hydrogenase active site, [Fe²⁺(CN⁻)₂(CO)Ni³⁺(SCH₂CH₃⁻)₄(OH⁻)(C₄NH₃CH₃)(H₂)]

